Journal of Applied Electrochemistry **32**: 481–486, 2002.

Electrochemical regeneration of chrome etching solution

Y. VAN ANDEL and L.J.J. JANSSEN
Department of Electrochemical Technology, Faculty of Chemical Engineering and Chemistry, Eindhoven University of Technology, PO Box 513, 5600 MB Eindhoven, The Netherlands

Received 28 August 2001; accepted in revised form 3 January 2002

Key words: boron-doped diamond, Cr(VI), Cr(III), oxidation

Abstract

A metal surface is chromatized with a chromic acid solution to obtain a good adherence of polymer coatings. In this process Cr(VI) is reduced to Cr(III). The oxidation strength of the solution decreases during use. The chrome solution needs to be regenerated and purified. A new anode material, namely boron-doped diamond, was used to investigate the oxidation of Cr(III) to Cr(VI). It was found that the current efficiency for Cr(III) oxidation decreases with increasing total current density. The current density of Cr(III) oxidation increases linearly with increasing Cr(III) concentration and is practically independent of the Cr(VI) concentration. It was concluded that the diffusion of Cr(III) is the rate-determining step for the Cr(III) oxidation at Cr(III) concentrations form 40 to 160 mol m^{-3}. The surface of the boron-doped diamond shows no signs of chemical corrosion or mechanical destruction. A filter-press type cell divided into two compartments by a cation exchange membrane was proposed. A cost calculation was carried out for the oxidation of 1.28 mmol s^{-1} Cr(III) in a 40 mol m^{-3} chrome(III) solution. Factors affecting the feasibility of this process include the costs of chemical waste disposal, the costs of chromic acid, government legislation and to a great extent the costs of the new anode material.

1. Introduction

Chromate conversion coatings are formed on metal surfaces by treating these with a chromic acid solution to guarantee paint adhesion. During this treatment the metal surface dissolves to a small extent causing a pH increase at the surface–liquid interface. This results in a deposit consisting of Cr(VI), Cr(III) and the coating metal itself [1]. Moreover, a large part of the Cr(III) and the coating metal ions enter the solution and the Cr(VI) concentration decreases. When the Cr(VI) concentration becomes too low and the Cr(III) concentration too high, the solution has to be replaced or regenerated.

To prevent the formation of large quantities of sludge and the high cost of sludge disposal, the spent chromatizing bath has to be regenerated and purified.

To remove metallic impurities from spent chrome plating baths, ceramic diaphragms have been proposed [2–4]. Since the chromate concentration in spent chromatizing baths is much smaller than that in spent chrome plating baths, commercial cation exchange membranes like Nafion® may be useful as separators in the cell to regenerate the spent chromatizing bath.

Lead dioxide is the only practical choice as anode material to oxidize Cr(III) to Cr(VI), where some oxygen evolution will occur as a competing reaction [5]. Also Bi-doped lead dioxide anodes have been proposed [6]. However, lead dioxide is subject to slow corrosion in the electrolysis conditions. Recently, highly promising boron-doped diamond anodes have become available. In this paper, experimental results on the efficiency of Cr(VI) formation for a spent chromatizing bath and Cr(III) model solutions are given. An economic evaluation is also presented.

2. Experimental details

2.1. *Electrolysis experiments*

During the electrolysis of Cr(III) solutions, two reactions take place at the anode under practical conditions forming Cr(VI) and oxygen. From the current efficiency for oxygen formation ϕ_{O_2}, the efficiency for Cr(III) oxidation, ϕ_{Cr}, was determined using $\phi_{Cr} = 1 - \phi_{O_2}$.

The electrolysis was carried out in a glass cell divided into two compartments by a cation exchange membrane (Nafion 117). Figure 1 represents the set-up schematically. The working electrode was placed inside the compartment on which a burette stood. At the start of experiments the burette was partly filled with the anolyte. During the electrolysis the liquid level inside the burette decreased because of oxygen gas formed at the anode. To calibrate the gas burette oxygen evolution experiments were carried out with a Pt anode in 1 M H_2SO_4, where the current efficiency for oxygen

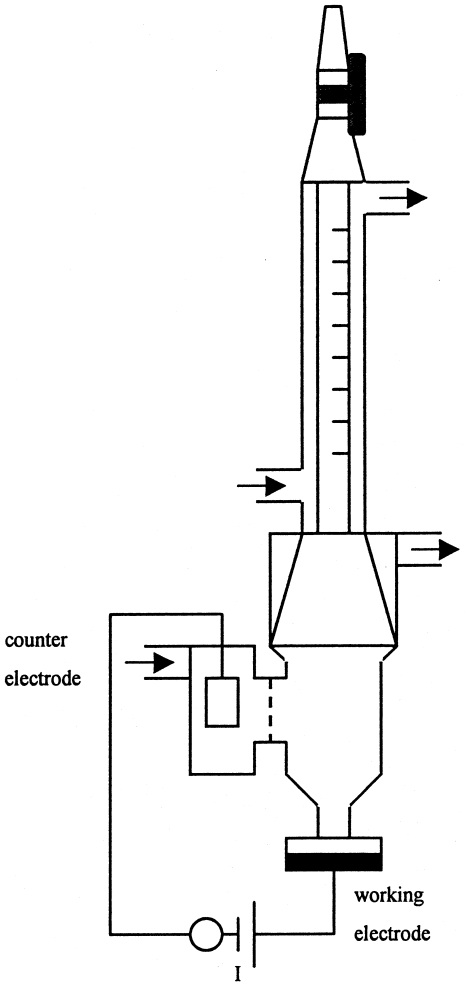

Fig. 1. Schematic arrangement of measurement of oxygen evolution rate.

evolution is practically 100%. The counter electrode was placed inside the other compartment, containing 1 M HNO_3 catholyte. Two types of working anode were used: namely, a boron-doped diamond sheet placed vertically in the centre of the anode compartment (not shown in Figure 1) and a boron-doped diamond electrode disc placed horizontally underneath the anode compartment. As a counter electrode a platinum sheet of 10 cm^2 was used.

The anode compartment consisted of two cylindrical parts of different diameter; the part with the biggest diameter was on top. At the connection between the two cylindrical parts, a funnel with a burette was placed so that the produced oxygen gas completely rose into the burette. Before starting the measurement, the solution was drawn into the burette until the desired level was reached. The produced oxygen gas lowered the liquid level in the burette. The amount of produced oxygen gas over a certain period was read from the drop of liquid level with time. This method is described in more detail elsewhere [7].

The current delivered by the power supply (Delta Elektronika, E030–1) was kept constant. The complete cell and burette were thermostrated. All experiments were performed at 25 °C.

2.2. *Voltammetric experiments*

Voltammetric experiments were carried out with an undivided cell with three electrodes. The working electrode was a flat boron-doped diamond sheet. The counter electrode was a flat platinum sheet and the reference electrode was a saturated calomel electrode (SCE). The measurements were performed using an Autolab potentiostat (Pgstat20, Ecochemie). The minimum potential of the scanning range was 0 V and the maximum potential varied from 3 to 4 V and the sweep rate was 20 mV s^{-1}. The electrode potential was corrected for the ohmic potential drop.

2.3. *Working electrodes*

Boron-doped diamond electrodes material was supplied by C.S.E.M. (Switzerland). Two types of boron-doped diamond electrodes were used (small rectangular sheets with an active electrode surface of 0.195 and 0.248 cm^2) and a disc with a diameter of 30 mm with only one active side. The material of the disc consisted of a silicon wafer of 1 mm thickness with a boron-doped diamond coating of 1 μm on one side of the wafer. To prevent too high currents a large part of the disc was covered with an insulating layer, so the electrode surface area was reduced to 0.090 cm^2. A platinum sheet was pressed against the reverse side of the disc electrode for current supply.

2.4. *Chrome solutions*

Experiments were done with an industrial solution and with model solutions. The industrial solution was taken from a finished chrome bath used in the zinc chromatizing process. It contained 0.23 M Cr(III), 0.48 M Cr(VI), 0.048 M HNO_3, 0.015 M HF, and small concentrations of Zn and Fe ions.

Two series of model solutions were used. Since the initial HNO_3 concentration in a chrome bath is equal to 0.1 M, this HNO_3 concentration was used for all model solutions. Series 1 solutions contained 0.1 M HNO_3, 0.13 M Cr(III) and various concentrations of Cr(VI) (0 to 0.5 M). Series 2 solutions contained 0.1 M HNO_3, 0.2 M Cr(VI), and various concentrations of Cr(III) (0 to 0.16 M). Cr(III) was added as $Cr(NO_3)_3$ and Cr(VI) as $Na_2Cr_2O_7$.

3. Results and discussion

3.1. *Electrolysis*

Figure 2 shows a typical result for the volume of evolved gas saturated with water, V_{O_2+w} as a function of time at a current density of 2.0 kA m^{-2}.

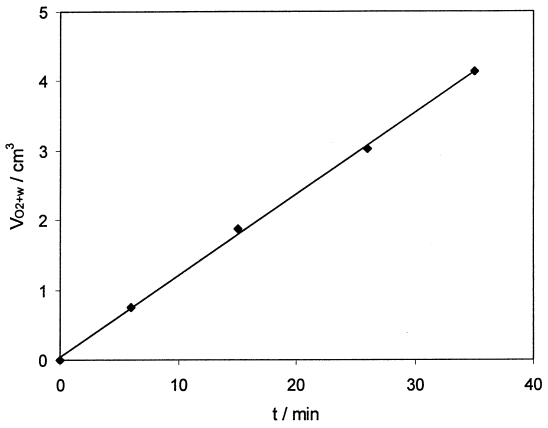

Fig. 2. Oxygen evolution rate against time at a current density of 2.0 kA m^{-2} on a boron-doped diamond electrode sheet of 0.248 cm^2 placed vertically in the industrial Cr(III) solution and at 25 °C.

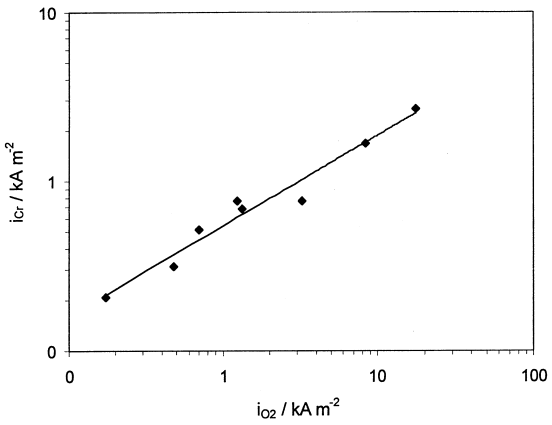

Fig. 4. i_{Cr} against i_{O_2} on a double logarithmic scale with boron-doped diamond electrode sheet of 0.248 cm^2 placed vertically in the industrial Cr(III) solution and at 25 °C.

A straight line describes the results. Its slope gives the rate of water saturated oxygen gas evolution, v_{O_2+w}. To obtain the oxygen evolution rate the water content is eliminated using

$$v_{O_2} = v_{O_2+w}\frac{P_{O_2+w} - P_w}{P_{O_2+w}}$$

From $P_w = 3 \times 10^3$ Pa and $P_{O_2+w} = 10^5$ Pa at 25 °C it follows that $v_{O_2} = 0.97\ v_{O_2+w}$.

From the oxygen evolution rate the current efficiency is calculated using

$$\phi_{O_2} = \frac{v_{O_2}}{v^*_{O_2}} \quad \text{with} \quad v^*_{O_2} = i_t A_e \frac{V_{M,O_2}}{nF}$$

where $v^*_{O_2}$ is the oxygen evolution rate at a current efficiency for oxygen of one.

Figure 3 shows the current efficiency for chromate formation as a function of current density. From this characteristic plot it is concluded that the current efficiency of Cr(III) oxidation decreases with increasing current density. It is likely that this decrease is caused by limitation of Cr(III) transfer to the electrode surface. It is well known that the rate of mass transfer strongly affects the rate of gas evolution [8].

To show this effect, i_{Cr} is plotted as a function of i_{O_2} double logarithmically in Figure 4. This is a straight line with a slope of 0.53. This value is almost equal to the value in [8] for the relation between the mass transfer coefficient of Ce(III) ions and the rate of oxygen evolution in 1 M H_2SO_4 solution for a vertical electrode.

To determine the effect of Cr(VI) concentration on the rate of Cr(III) oxidation, electrolyses were carried out with model solutions of varying Cr(VI) concentration. Figure 5 shows the results. When taking into account the spread in the experimental results it follows from Figure 5 that the Cr(VI) concentration does not affect the rate of chromate formation.

To determine the effect of Cr(III) concentration on the rate of Cr(III) oxidation, electrolyses were carried out at total current densities where the current density for the oxygen evolution was around 800 A m^{-2}. Since the total current density is adjusted, generally i_{O_2} deviated a little

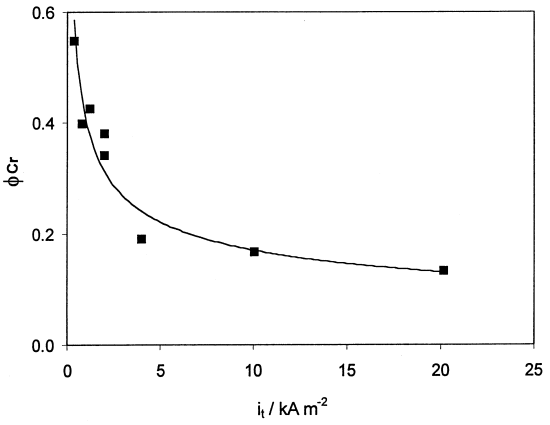

Fig. 3. Current efficiency of chrome(III) oxidation as a function of total current density for a boron-doped diamond electrode sheet of 0.248 cm^2 placed vertically in the industrial Cr(III) solution and at 25 °C.

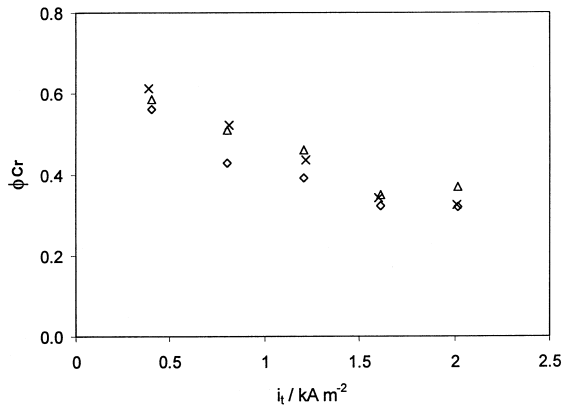

Fig. 5. Current efficiency of chrome(III) oxidation as a function of total current density for a vertically placed boron-doped diamond electrode (0.248 cm^2) in model solutions with 0.13 M Cr(III), 0.1 M HNO_3 and 0 M (×), 0.1 M (◇), and 0.5 M (△) Cr(VI) and at 25 °C.

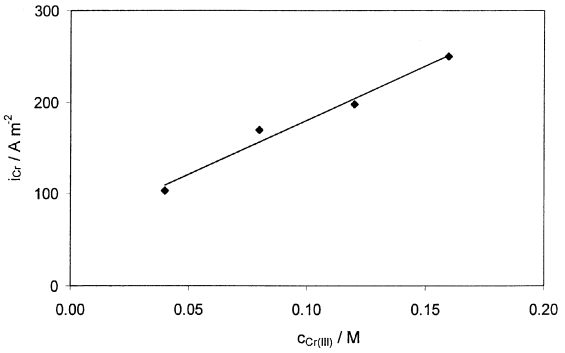

Fig. 6. i_{Cr} against Cr(III) concentration at $i_{O_2} = 800$ A m^{-2} for a vertically placed boron-doped diamond electrode in model solutions with 0.2 M Cr(VI), 0.1 M HNO_3 and various Cr(III) concentrations and at 25 °C.

from 800 A m^{-2}. The effect of this deviation was taken into account using the proportionality between i_{Cr} and $i_{O_2}^{0.53}$ to obtain the current density i_{Cr} at $i_{O_2} = 800$ A m^{-2} as a function of Cr(III) concentration. The results are given in Figure 6.

The results show that the rate of Cr(III) oxidation increases linearly with the Cr(II) concentration, independent of the Cr(VI) concentration and increases linearly with $i_{O_2}^{0.53}$. It can be concluded that in the dilute Cr(III) solutions diffusion of Cr(III) ions is the rate-determining step for the chromate formation.

3.2. *Voltammograms*

A typical voltammogram for a horizontal boron-doped diamond electrode in the industrial chromate solution is given in Figure 7. The direction of the potential scan has practically no effect on the voltammogram. From this Figure

$$E = 1.76 + 0.245 \log i_t$$

where i_t is expressed in A m^{-2}.

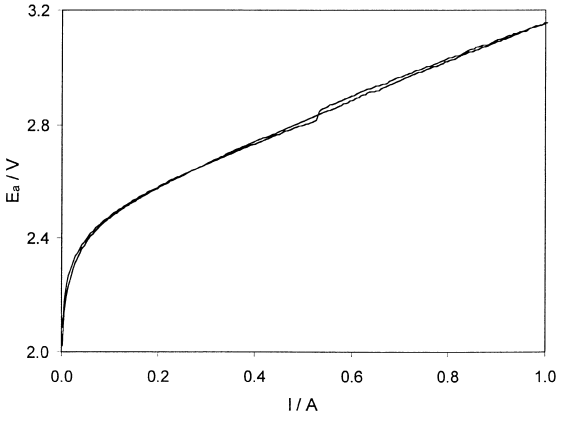

Fig. 7. Voltammogram for a boron-doped diamond electrode disc in the industrial Cr(III) solution and at 25 °C and a sweep rate of 20 mV s^{-1}.

4. Cell design and correlations

4.1. *Cell design*

To ensure a constant composition of a chromatizing bath, a continuous regeneration process is proposed. The solution is pumped from the chromatizing bath through a regeneration unit consisting of electrolysis cells. This unit can be considered as a batch-recirculation reactor, where the cell is a plug flow reactor and the chromatizing bath a continuously stirred tank reactor. The aim is to keep the Cr(III) concentration and the Cr(VI) concentration of a 0.2 m^3 chromatizing bath on 40 and 80 mol m^{-3}, respectively, at a Cr(VI) conversion rate of 1.28×10^{-3} mol s^{-1} in the chromatizing bath.

Boron-doped diamond electrodes are only commercially available as flat plates and it is assumed that a dimension of 50×50 cm^2 will be attainable in the near future.

In this case the well-known filter press cell is the appropriate choice. This cell has to be divided into two compartments by a cation exchange membrane to prevent reduction of Cr(VI) at the cathode and to remove metal ions originated from the chromatized material. The dimensions of both the anode and cathode compartment are 50 cm in height, 50 cm in width and 1 cm in thickness, because of the limited size of diamond electrodes.

4.2. *Cell correlations*

4.2.1. *Mass transfer coefficient*

During the regeneration of the chromatizing bath under industrial conditions oxygen evolution also takes place. Its rate will effect significantly the rate of mass transfer of Cr(III) ions to the diamond anode. The mass transfer coefficient of combined forced liquid convection and gas evolution is described [9] by the empirical relation:

$$k_t^2 = k_c^2 + k_g^2 \tag{1}$$

where $k_g = a i_{O_2}^b$ and from Figure 4. It follows that $a = 4.4 \times 10^{-7}$ A m^{-2} and $b = 0.53$.

In electrolysis cells under industrial conditions the solution flow rate is usually lower than 1.0 m s^{-1} [2]. It can be shown that the solution flow is laminar at $v_s < 0.2$ m s^{-1} and is in the transition from laminar to turbulent at 0.2 m s^{-1} $< v_s <$ 2 m s^{-1}.

The Sherwood number for fully developed laminar flow [10] is

$$Sh = 1.85\, Re^{1/3} Sc^{1/3} (d_e/L_e)^{1/3} \tag{2}$$

and for the transition range [11]

$$\frac{Sh}{Sc^{1/3}} = -5.8910^{-8}\, Re^2 + 4.57 \times 10^{-3}\, Re - 3.02 \tag{3}$$

where $Re = d_e v_s / v_s$, $Sc = v_s / D$ and $Sh = k_c d_e / D$

4.2.2. *Cr(III) oxidation*

Design equations for a plug flow reactor are well described [10]. Under complete mass transfer control and by definition of the mass transfer coefficient

$$k_t = i_g/nF_{c_b} \tag{4}$$

it can be shown that:

$$c_{out} = c_{in} \exp[-(k_t A_e/N_s)] \tag{5}$$

where $N_s = v_s d_{m-a} W_e$ (6)

The bulk concentration of Cr(III) decreases with increasing distance from the cell inlet, since on the anode Cr(III) is converted to Cr(VI). From results for the distribution of mass transfer over a 0.5 m tall vertical hydrogen evolving electrode [12] it is likely that the Cr(III) mass transfer coefficient k_t decreases very slightly for the topmost 0.4 m of the working electrode. In vertical gas evolving electrolyses the current density decreases only slightly with increasing height, in particular at low gas voidages [13]. From [12, 13] it follows that the local limiting current density for Cr(III) oxidation will be given by a very complex correlation of many parameters, that is, $c_{Cr(III)}$, k_t, i_{O_2} and v_s. As a first approach it is assumed that i_t, $i_{g,Cr}$ and i_{O_2} are constant over the whole cell height, where $i_{g,Cr}$ is calculated using Equations 1–4 at the Cr(III) concentration at the cell inlet.

Figure 8 shows the relation between $i_{g,Cr}$ and i_{O_2} at $c_{Cr(III)}$=40 mol m^{-3} for natural convection and at a solution flow rate of 1 m s^{-1}.

Assuming v_s has to be smaller than 1 m s^{-1} and i_t smaller than 2.5 kA m^{-2} it can be shown that at least four cells in parallel configuration are needed to oxidize 1.28×10^{-3} mol s^{-1} Cr(III) to Cr(VI), corresponding to $I_{Cr} = 370$ A. Calculations have also been carried out for cells in serial configuration [4]. It has been found that the electrolysis power consumption is smaller for the parallel than the serial configuration; therefore the serial configuration is not discussed extensively in this paper.

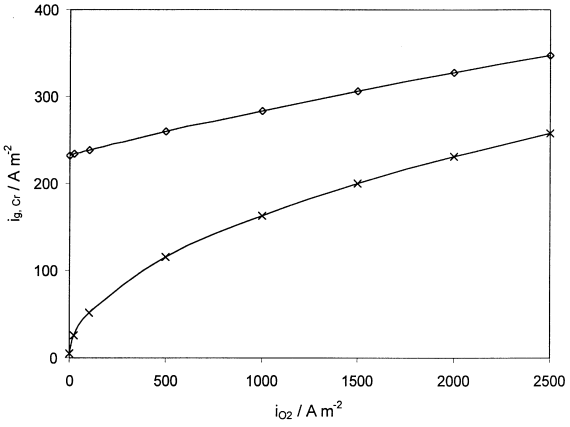

Fig. 8. Calculated relation between $i_{g,Cr}$ and i_{O_2}, at natural convection $v_s = 0$ m s^{-1} (×) and at a flow rate of 1 m s^{-1} (◇).

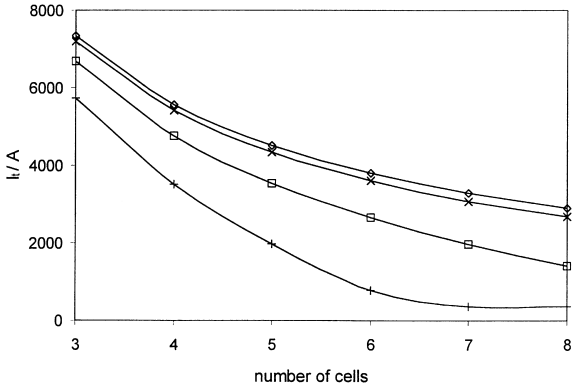

Fig. 9. Total current as a function of the number of cells at $I_t = 370$ A and 40 mol m^{-3} Cr(III) solution for several flow rates 0.1 (◇), 0.2 (×), 0.5 (□) and 1.0 m s^{-1} (+).

In Figure 9 the total current I_t and in Figure 10 the current efficiency for Cr(III) oxidation ϕ_{Cr} are given for various numbers of cells in parallel configuration at a Cr(III) concentration of 40 mol m^{-3} and $I_{Cr} = 370$ A.

From Figure 10 it follows that no oxygen gas is evolved using more than seven cells at $v_s = 1.0$ m s^{-1}. The model shows that for $I < I_{g,Cr}$ only Cr(III) ions are oxidized. Also at high solution flow rates the current efficiency for Cr(III) reduction has to be smaller than 1, since the limiting current density for Cr(III) oxidation occurs in the potential range where oxygen gas is also formed. This Figure also shows a clear effect of the solution flow rate; so both I_{O_2} and I_t decrease with increasing number of cells and solution flow rate.

4.2.3. *Cell voltage and total power*

The cell voltage was calculated as a function of total current density at 25 °C for the cell with spent solution as anolyte and 1 M H_2SO_4 as catholyte and a cation exchange membrane with a specific resistance of 1.67×10^{-4} Ω m^2. The cell voltage E_{cell} as a function of the number of cells in the parallel configuration is plotted in Figure 11 at various solution flow rates. The results for the total costs are given in Figure 12. At a solution flow rate equal to and smaller than 1 m s^{-1} the

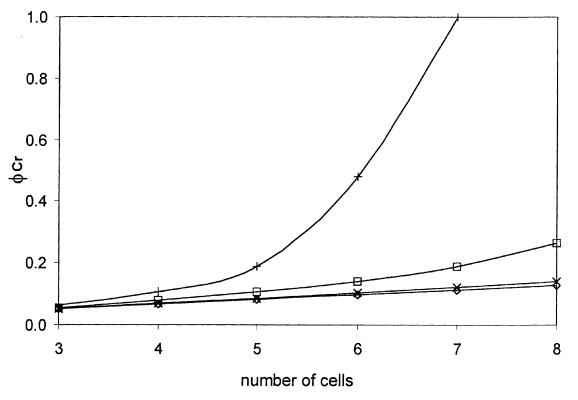

Fig. 10. Current efficiency of chrome(III) oxidation as a function of the number of cells at $I_t = 370$ A and 40 mol m^{-3} Cr(III) solution for several flow rates 0.1 (◇), 0.2 (×), 0.5 (□) and 1.0 m s^{-1} (+).

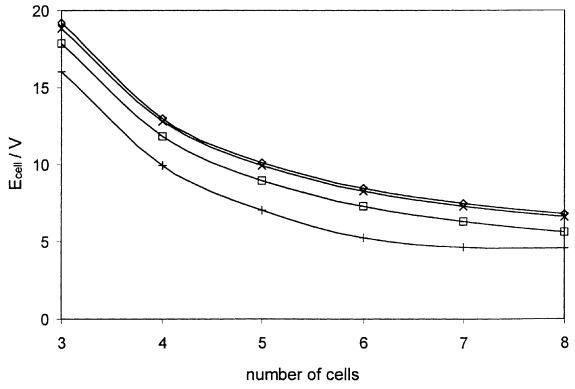

Fig. 11. Cell voltage as a function of the number of cells at $I_t = 370$ A and 40 mol m^{-3} Cr(III) solution for several flow rates 0.1 (◇), 0.2 (×), 0.5 (□) and 1.0 m s^{-1} (+).

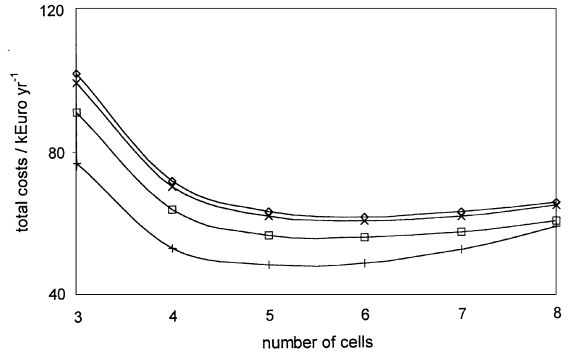

Fig. 12. Total costs as a function of the number of cells at $I_t = 370$ A and 40 mol m^{-3} Cr(III) solution for several flow rates 0.1 (◇), 0.2 (×), 0.5 (□) and 1.0 m s^{-1} (+).

pumping power is much smaller than the electrolysis power [14] and can be neglected.

5. Economic evaluation

To build a regeneration plant, divided cells, a power supply, an anolyte pump and a catholyte pump and two solution reservoirs are needed. For a plant consisting of four cells the purchased costs for the anodes is about 80% of the total purchased costs for the plant [14], assuming that the purchased costs for the diamond anode per m^2 is given by 12 700 $A_e^{-0.27}$ Euro, where A_e is the anode surface area in m^2.

Details of the purchased costs, capital costs and variable costs are given in [14]. The total costs are the sum of the capital and the variable costs. Figure 12 gives the total costs per year as a function of the number of cells at $I_t = 370$ A and a bulk Cr(III) concentration of 40 mol m^{-3} and at various solution flow rates. In this case the results indicate a minimum of total costs for a regeneration unit consisting of six cells. The minimum total costs decreases strongly with increasing solution flow rate.

Using a stack of six cells it was found that in this case at a solution flow rate of 1 m s^{-1} the capital costs are about the half of the total costs, being 56 000 Euro. It can be concluded that the economic possibilities for this regeneration process depend strongly on the price of boron-doped diamond anodes.

A decrease in anode price gives a decrease in both capital and variable costs and the regeneration process becomes more attractive.

6. Conclusions

(i) Under industrial conditions the oxidation of chrome(III) is limited by its transport to the boron-doped diamond anode.
(ii) The mass transfer coefficient for chrome(III) is determined by the rate of oxygen evolution as well as the solution flow rate.
(iii) A stack of filter press cells in parallel configuration is proposed as regeneration plant.
(iv) The number of cells has been calculated for a fixed rate of chrome(III) oxidation, where a maximum solution flow rate of 1 m s^{-1}, generally acceptable under industrial conditions, is taken into account.
(v) The economic evaluation shows that the price of boron-doped diamond electrodes is most determining for the industrial application of this regeneration process.

References

1. F.A. Lowenheim, 'Modern Electroplating' (J. Wiley & Sons, New York, 3rd Edition, 1974) p. 77.
2. N.V. Mandich, C-C. Lee and J.R. Selman, *Plat. Surf. Finish.* **84** (12) (1997) 82.
3. S.L. Guddati, T.M. Holsen, C-C. Li, J.R. Selman and N.V. Mandich, *J. Appl. Electrochem.* **29** (1999) 1129.
4. K. Mondal, N.V. Mandich and S.B. Lalvani, *J. Appl. Electrochem.* **31** (2001) 165.
5. D. Pletcher, 'Industrial Electrochemistry' (Chapman & Hall, London, 1982), p. 149.
6. K.L. Pamplin and D.C. Johnson, *J. Electrochem. Soc.* **143** (1996) 2119.
7. L.J.J. Janssen and P.D.L. van der Heyden, *J. Appl. Electrochem.* **25** (1995) 126.
8. L.J.J. Janssen and J.G. Hoogland, *Electrochim. Acta* **15** (1970) 1013.
9. L.J.J. Janssen, *J. Appl. Electrochem.* **17** (1989) 1188.
10. D. Pletcher and F.C. Walsh, '*Industrial Electrochemistry*' (Blackie Academic and Professional, London, 2nd edn, 1993).
11. D.Q. Kern, 'Process Heat Transfer' (McGraw-Hill, London, 1950).
12. H.F.M. Gijsbers and L.J.J. Janssen, *J. Appl. Electrochem.* **19** (1989) 637.
13. L.J.J. Janssen and G.J. Visser, *J. Appl. Electrochem.* **21** (1991) 753.
14. Y. Van Andel, Report, Eindhoven University of Technology, 2001.